Intraindividual Comparison of ^{18}F-PSMA-1007 with Renally Excreted PSMA Ligands for PSMA PET Imaging in Patients with Relapsed Prostate Cancer

Felix Dietlein[1,2], Carsten Kobe[1], Melanie Hohberg[1], Boris D. Zlatopolskiy[3], Philipp Krapf[4], Heike Endepols[1,3], Philipp Täger[1], Jochen Hammes[1], Axel Heidenreich[5], Thorsten Persigehl[6], Bernd Neumaier[3,4], Alexander Drzezga*[1], and Markus Dietlein*[1]

[1]Department of Nuclear Medicine, University Hospital of Cologne, Cologne, Germany; [2]Department of Medical Oncology, Dana-Farber Cancer Institute, Harvard Medical School, Boston, Massachusetts; [3]Institute of Radiochemistry and Experimental Molecular Imaging, University Hospital of Cologne, Cologne, Germany; [4]Institute of Neuroscience and Medicine, INM-5: Nuclear Chemistry, Forschungszentrum Jülich GmbH, Jülich, Germany; [5]Department of Urology, University Hospital of Cologne, Cologne, Germany; and [6]Institute of Diagnostic and Interventional Radiology, University Hospital of Cologne, Cologne, Germany

^{18}F-prostate-specific membrane antigen (PSMA)-1007 is excreted mainly through the liver. We benchmarked the performance of ^{18}F-PSMA-1007 against 3 renally excreted PSMA tracers. **Methods:** Among 668 patients, we selected 27 in whom PET/CT results obtained with ^{68}Ga-PSMA-11, ^{18}F-DCFPyL (2-(3-(1-carboxy-5-[(6-[^{18}F]fluoro-pyridine-3-carbonyl)-amino]-pentyl)-ureido)-pentanedioic acid), or ^{18}F-JK-PSMA-7 (JK, Juelich-Koeln) were interpreted as equivocal or negative or as oligometastatic disease (PET-1). Within 3 wk, a second PET scan with ^{18}F-PSMA-1007 was performed (PET-2). The confidence in the interpretation of PSMA-positive locoregional findings was scored on a 5-point scale, first in routine diagnostics (reader 1) and then by an independent second evaluation (reader 2). Discordant PSMA-positive skeletal findings were examined by contrast-enhanced MRI. **Results:** For both readers, ^{18}F-PSMA-1007 facilitated the interpretability of 27 locoregional lesions. In PET-2, the clinical readout led to a significantly lower number of equivocal locoregional lesions ($P = 0.024$), and reader 2 reported a significantly higher rate of suspected lesions that were falsely interpreted as probably benign in PET-1 ($P = 0.023$). Exclusively in PET-2, we observed a total of 15 PSMA-positive spots in the bone marrow of 6 patients (22%). None of the 15 discordant spots had a morphologic correlate on the corresponding CT scan or on the subsequent MRI scan. Thus, ^{18}F-PSMA-1007 exhibits a significantly higher rate of unspecific medullary spots ($P = 0.0006$). **Conclusion:** ^{18}F-PSMA-1007 may increase confidence in interpreting small locoregional lesions adjacent to the urinary tract but may decrease the interpretability of skeletal lesions.

Key Words: prostate cancer; PET; PSMA tracer; ^{18}F-PSMA-1007; ^{68}Ga-PSMA-11; ^{18}F-DCFPyL; ^{18}F-JK-PSMA-7

J Nucl Med 2020; 61:729–734
DOI: 10.2967/jnumed.119.234898

Prostate-specific membrane antigen (PSMA) PET/CT imaging is widely used for tumor localization in biochemical recurrence of prostate cancer. A broad spectrum of PSMA ligands is now clinically available, including ^{68}Ga-PSMA-11, ^{18}F-DCFPyL (2-(3-(1-carboxy-5-[(6-[^{18}F]fluoro-pyridine-3-carbonyl)-amino]-pentyl)-ureido)-pentanedioic acid), ^{18}F-JK-PSMA-7 (JK, Juelich-Koeln), and ^{18}F-PSMA-1007 (*1–6*). ^{18}F-JK-PSMA-7 is the PSMA-specific derivative 2-Methoxy(MeO)-^{18}F-DCFPyL and proved noninferior to ^{68}Ga-PSMA-11 in an intraindividual pilot study (*6,7*).

Most of the currently available PSMA tracers used for PET/CT imaging are excreted through the kidneys, thus leading to a high background signal in the urinary tract. It can therefore occasionally be difficult to differentiate between urine retention in the ureter and small adjacent pelvic lymph nodes. This ambiguity limits the reader's confidence in interpreting small PSMA-positive lesions close to the urinary tract as tumor relapse. Similarly, local recurrence close to the urinary bladder can easily be confused with urinary activity. Resolving this intrinsic limitation would bring us a step further toward exploiting the full potential of PSMA tracers.

Recently, the tracer ^{18}F-PSMA-1007 was introduced into clinical practice (*1,2*). In contrast to other PSMA tracers, ^{18}F-PSMA-1007 is excreted primarily through the liver. A pharmacodynamic study demonstrated that during the first 2 h, only 1%–2% of the injected ^{18}F-PSMA-1007 activity was eliminated in the urine (*1*). Considerable hope is therefore being placed on ^{18}F-PSMA-1007 as a means of resolving the limited interpretability of PSMA-positive lesions near the urinary tract. A recent pilot study involving intraindividual comparisons reported that ^{18}F-PSMA-1007 and ^{18}F-DCFPyL detected the same lesions in 12 patients examined at initial staging (*8*).

Here, we present an intraindividual comparison of ^{18}F-PSMA-1007 with ^{68}Ga-PSMA-11, ^{18}F-DCFPyL, and ^{18}F-JK-PSMA-7 in 27 patients. We compared the readers' confidence in interpreting PSMA-positive lesions as tumor lesions, focusing on the interpretability of locoregional lesions near the urinary tract. Additionally, we evaluated the performance of ^{18}F-PSMA-1007 in the whole-body PET scan.

MATERIALS AND METHODS

Indication for PET/CT

Most patients (23/27) were referred for PET/CT imaging because of biochemical recurrence according to the following criteria: a

Received Aug. 9, 2019; revision accepted Sep. 20, 2019.
For correspondence or reprints contact: Markus Dietlein, Department of Nuclear Medicine, University Hospital of Cologne, Kerpener Strasse 62, 50937 Cologne, Germany.
E-mail: markus.dietlein@uk-koeln.de
*Contributed equally to this work.
Published online Oct. 18, 2019.

prostate-specific antigen (PSA) increase to 0.2 μg/L or more after prostatectomy (R0 or R1 resection) and a PSA increase of at least 2.0 μg/L above the nadir after radiotherapy, as determined by the referring urologist. One patient had a persistent PSA level after prostatectomy. Additionally, we included 2 patients with oligometastatic disease and 1 patient with secondary neoplasia (rectal cancer) for tissue differentiation. None of these patients received androgen deprivation therapy.

Tracer Preparation

^{18}F-PSMA-1007 was synthesized on demand at the Research Center Juelich using a method previously described by Giesel et al. (*1*). All tracers were produced in accordance with applicable good manufacturing practices (*7*). The 11 batches of ^{18}F-PSMA-1007 for our 27 patients were produced at an average activity of 10.11 ± 3.76 GBq, a specific activity of 318.09 ± 235.15 GBq/μmol, an activity concentration of 986.91 ± 358.97 MBq/mL, and a radiochemical purity of 99.0% ± 0.77%. Synthesis of ^{68}Ga-PSMA-11 (*9*), ^{18}F-DCFPyL (*7,10*), and ^{18}F-JK-PSMA-7 (*7*) was performed as described previously.

Verification of Locoregional PSMA-Positive Lesions

We followed up on the 19 patients with locoregional PSMA-positive lesions to confirm that these lesions had a clinical correlate. For 5 patients, a histology report after salvage lymphadenectomy (3 patients) or salvage prostatectomy (1 patient) or biopsy (1 patient) was available. These histology reports directly verified the PSMA-positive lesions on the PET scan as prostate cancer tissue. For another 11 patients, follow-up data including PSA levels were available, and we observed a decrease in the PSA level after radiotherapy (9 patients) or an increase in the PSA level in combination with progressive disease on a subsequent PSMA PET/CT scan after watchful waiting (2 patients). We cross-validated the PSMA-positive lesions with an MRI scan of the pelvis in 1 patient. Follow-up data were not available for the remaining 2 patients. These 2 patients (patients 8 and 19 in Supplemental Table 1; supplemental materials are available at http://jnm.snmjournals.org) had previously undergone at least 2 PET scans and had already been irradiated for PSMA-positive locoregional recurrences. The PSMA-positive lesions in PET-1 and PET-2 were localized in these irradiated regions. Given this history, we found the PSMA-positive PET findings plausible.

Patient Characteristics

This observational study was approved and conducted in compliance with the Institutional Review Board. All patients gave their written informed consent to PET imaging and inclusion of their data in a retrospective analysis. All procedures were performed in compliance with the regulations of the responsible local authorities (District Administration of Cologne, Germany).

Patients with relapsed prostate cancer underwent PET/CT imaging with one of our routinely used PSMA tracers, ^{68}Ga-PSMA-11, ^{18}F-DCFPyL, or ^{18}F-JK-PSMA-7, as part of their clinical workup. A second PET/CT scan with ^{18}F-PSMA-1007 was performed in 27 cases (average age, 67.2 ± 7.8 y) for 1 of the following 3 reasons: the first PET scan was completely PSMA-negative; the first PET scan exhibited a PSMA-positive spot near the ureter, urethra, or bladder that was interpreted as equivocal; or the first PET scan revealed a single suspected lesion before metastasis-directed therapy (e.g., radiotherapy). The second PSMA PET/CT scan with ^{18}F-PSMA-1007 PET/CT was performed within 3 wk after the first scan. The 27 patients were selected from an overall group of 668 patients who received PSMA PET/CT within the 12-mo period of recruitment from April 2017 to March 2018. More details on patient characteristics are given in Supplemental Table 1.

Imaging and Reading

We performed PET/low-dose CT imaging using standard activities and intervals between the injection and the start of data acquisition, as recommended for ^{68}Ga-PSMA-11 (n = 16; average dosage, 159 ± 31 MBq), ^{18}F-DCFPyL (n = 5, 343 ± 52 MBq), and ^{18}F-JK-PSMA-7 (n = 6, 323 ± 54 MBq) (*4–6*). As in previous studies on ^{18}F-PSMA-1007 (*1,3*), we acquired ^{18}F-PSMA-1007 scans 2 h after tracer injection with an average dose of 343 ± 49 MBq. All images were acquired on a Biograph mCT 128 Flow PET/CT scanner (Siemens Healthineers). The same filters and acquisition times (flow motion bed speed of 1.5 mm/s) were used for the 4 PSMA ligands. Images were reconstructed using an ultra-high-definition algorithm.

A team of specialists in routine diagnostics (2 specialists in nuclear medicine and 1 radiologist, "reader 1") and 1 added reader ("reader 2") independently interpreted each PET/CT scan according to the criteria for harmonization of PSMA PET/CT interpretation (*11*). Reader 2 reevaluated the PET scans without knowledge of the clinical data or the MRI findings 3–15 mo after the initial reading. We used the 5-point PSMA-RADS (reporting and data system) scale (version 1.0) to score the interpretability of each PSMA-positive lesion based on these reports. In particular, we classified each PSMA-positive finding as benign (PSMA-RADS-1), likely benign (PSMA-RADS-2), equivocal (PSMA-RADS-3), likely malignant (PSMA-RADS-4), or certainly malignant (PSMA-RADS-5) (*12*).

Equivocal PSMA-positive lesions in the bone marrow were examined by dedicated, contrast-enhanced MRI scans. MRI was performed on 1.5-T and 3.0-T MR scanners (Achieva and Ingenia; Philips Healthcare) using the clinical standard protocol by application of 0.1 mmol of gadolinium-DOTA per kilogram of body weight (Clariscan; GE Healthcare). Spine sequences were sagittal T2-weighted, sagittal short T2-weighted inversion recovery (STIR), sagittal T1-weighted imaging before and after contrast injection and postprocessing subtraction, and sequential transversal T2-weighted and T1-weighted spectral presaturation with inversion recovery. Pelvic sequences were transversal STIR, transversal diffusion-weighted whole-body imaging with background body signal suppression, coronal STIR, coronal T1-weighted imaging before and after contrast injection, and transversal T1-weighted multiple-echo Dixon fat suppression.

Statistics

Statistical analyses were performed with Microsoft Excel, the R programming language, and the programs on vassarstats.net. We used the Fisher exact test (2 × 2 contingency tables), the Freeman–Halton extension (3 × 2 contingency tables) of the Fisher exact test, and the Wilcoxon signed-rank test to compare groups. To compare the shift in RADS categories, we combined categories 1 (almost certainly benign) and 2 (likely benign), as well as categories 4 (likely malignant) and 5 (almost certainly malignant), to obtain 3 × 2 contingency tables The interobserver variability was tested by the weighted Cohen κ-test.

RESULTS

Interpretability of Locoregional PSMA-Positive Lesions

We performed ^{18}F-PSMA-1007 PET on 27 patients who had been examined with ^{68}Ga-PSMA-11 (n = 16), ^{18}F-DCFPyL (n = 5), or ^{18}F-JK-PSMA-7 (n = 6) less than 3 wk previously (Figs. 1–3; Supplemental Figs. 1–4). For 8 of these 27 patients, the first PET exam did not reveal any locoregional lesions. In these 8 patients, the second scan with ^{18}F-PSMA-1007 was negative in the locoregional region as well (7 patients were entirely negative, one patient had an additional PSMA-positive bone marrow lesion on PET-1 and PET-2).

The remaining 19 patients were finally diagnosed with a PSMA-positive locoregional tumor relapse when all imaging procedures were completed. In total, we identified 27 PSMA-positive locoregional lesions in these patients. We then examined how interpretable these 27 PSMA-positive lesions were in both corresponding PET scans (PET-1: ^{68}Ga-PSMA-11, ^{18}F-DCFPyL,

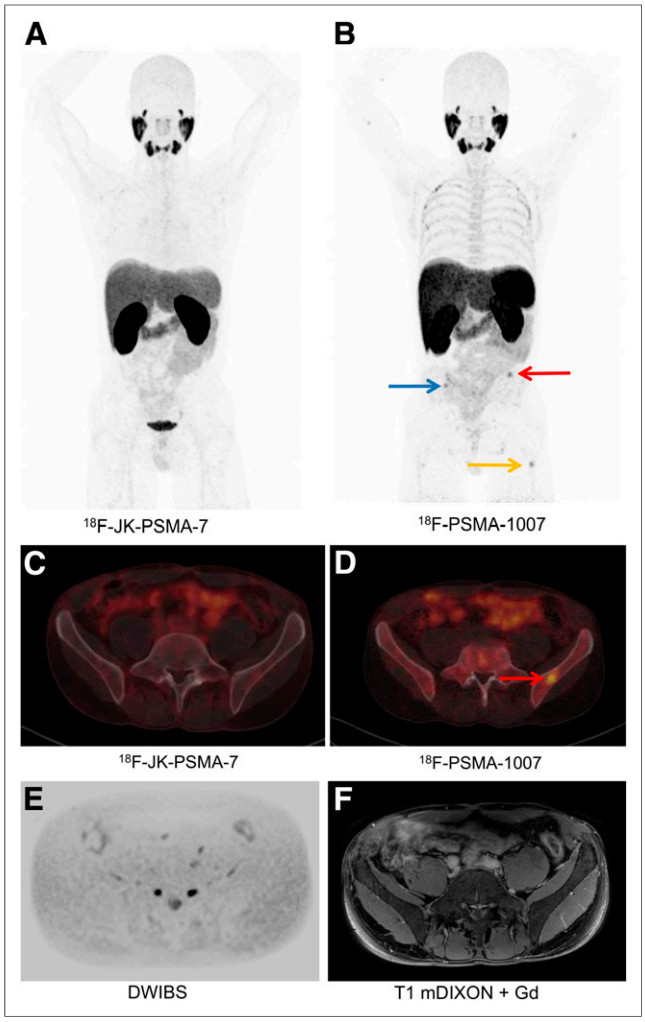

FIGURE 1. ^{18}F-JK-PSMA-7 PET/low-dose CT (A and C) and ^{18}F-PSMA-1007 PET/low-dose CT (B and D) images in patient 21, with biochemical recurrence. Histologically confirmed PSMA-positive lesion in right seminal vesicle is shown in Supplemental Figure 1. Osteomedullary spots with ^{18}F-PSMA-1007 in left os ilium (red arrows in B and D), in right os ilium (blue arrow in B), and in left femur (orange arrow in B) did not have any correlate on MRI scan (E and F). Salvage prostatectomy produced excellent PSA response. DWIBS = diffusion weighted whole body imaging with background body signal suppression; mDIXON FS = multiple-echo Dixon fat suppression.

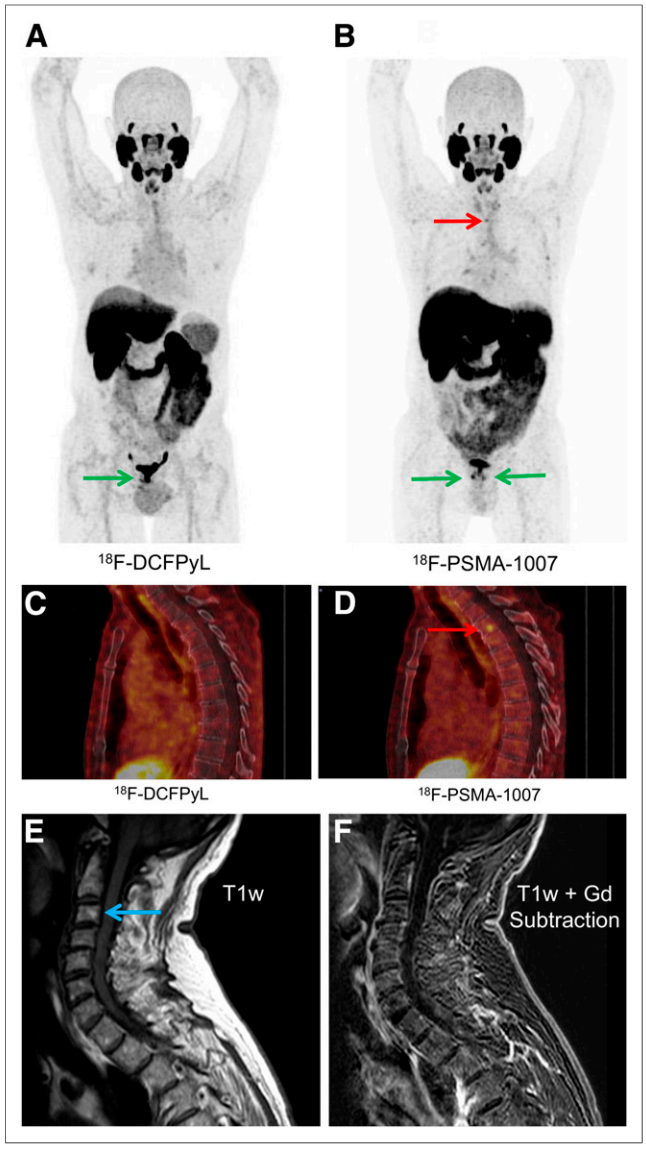

FIGURE 2. ^{18}F-DCFPyL PET/low-dose CT (A and C) and ^{18}F-PSMA-1007 PET/low-dose CT (B and D) images in patient 13, with biochemical recurrence. PSMA-positive intraprostatic lesions in left and right lobes of prostate are visible with both ^{18}F-DCFPyL and ^{18}F-PSMA-1007 (green arrows). Osteomedullary spots in thoracic spine (T3, red arrows) did not have any correlate on MRI scan (E and F). Hemangioma in C3 was PSMA-negative (blue arrow). T1w = T1-weighted.

or ^{18}F-JK-PSMA-7; PET-2: ^{18}F-PSMA-1007). Reader 1 interpreted 15 of 27 lesions on PET-1 as equivocal (PSMA-RADS-3), whereas the fraction of equivocal lesions on PET-2 was significantly lower (6/27 lesions, $P = 0.024$, Fisher exact test). For both readers, the rate of PSMA-positive lesions that were falsely interpreted as benign was lower on PET-2 (reader 1: 0/27, reader 2: 0/27) than on PET-1 (reader 1: 3/27, reader 2: 6/27), and this difference reached statistical significance for reader 2 ($P = 0.023$). The rate of equivocal lesions did not differ significantly between the 2 scans for reader 2 (6 vs. 5 lesions, $P = 1.0$). Overall, ^{18}F-PSMA-1007 exhibited a significant shift in PSMA-RADS categories toward higher confidence both for reader 1 (lower rate of equivocal ratings, $P = 0.00154$, Freeman–Halton extension of Fisher exact test) and for reader 2 (lower rate of falsely benign interpreted lesions, $P = 0.01745$) (Table 1), suggesting that ^{18}F-PSMA-1007 enhanced the confidence in interpretation of locoregional PSMA-positive lesions for both independent readers.

The ^{18}F-PSMA-1007 PET scan (PET-2) resulted in almost perfect agreement ($\kappa = 0.95$, weighted Cohen kappa), whereas the interpretation of PET-1 led to moderate agreement between the clinical readout and reader 2 ($\kappa = 0.49$; weighted Cohen kappa). The data are shown in Supplemental Table 2.

We next examined which aspects might have contributed to this improved interpretability. Concordantly, with the help of PET-2, both readers corrected 2 false-positive PET-1 interpretations of pelvic PSMA spots (no. 2 and 24; Supplemental Table 1) that were PSMA-negative on PET-2. Furthermore, the signal (SUV_{max}) of the 24 PSMA-positive lesions was significantly higher ($P = 0.00178$,

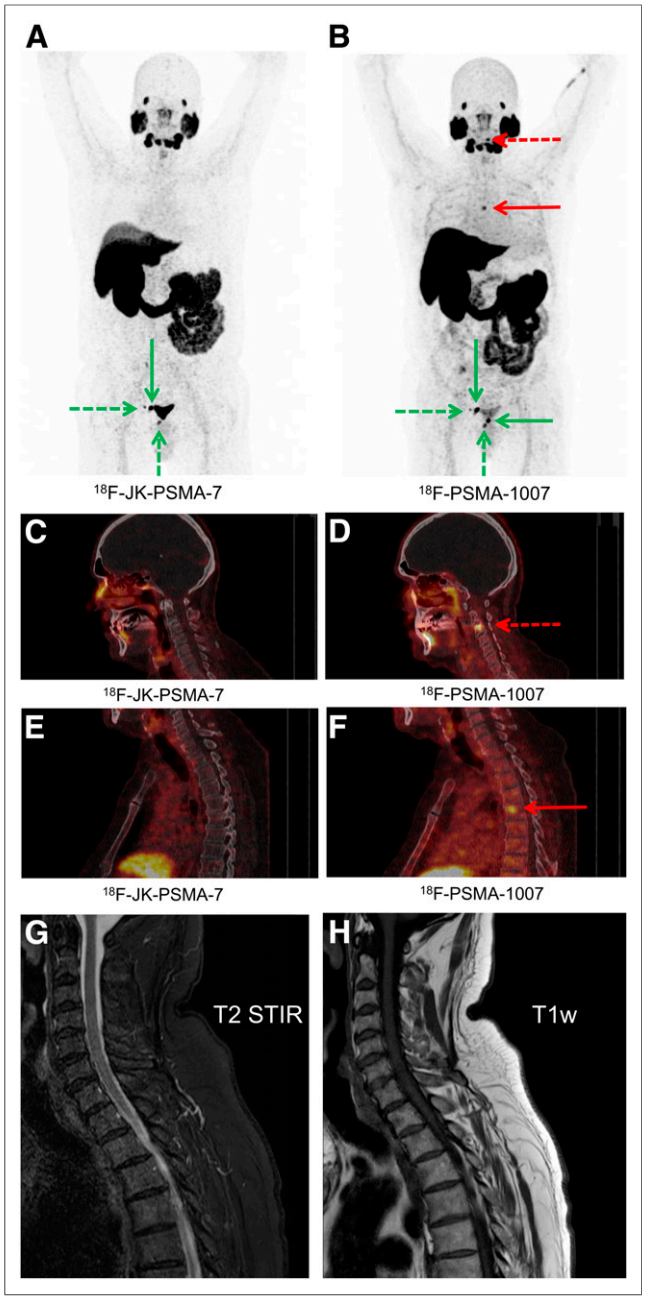

FIGURE 3. ^{18}F-JK-PSMA-7 PET/low-dose CT (A, C, and E) and ^{18}F-PSMA-1007 PET/low-dose CT (B, D, and F) images in patient 27, with biochemical recurrence. Maximum-intensity projections with ^{18}F-JK-PSMA-7 and ^{18}F-PSMA-1007 show 2 PSMA-positive right iliac lymph nodes and PSMA-positive relapse below bladder. Additionally, ^{18}F-PSMA-1007 PET scan in B shows further relapse at junction between bladder and urethra. Osteomedullary spots in cervical spine (C3, dashed red arrows in B and D) and thoracic spine (T5, solid red arrows in B and F) did not have any correlate on MRI scan (G and H).

Wilcoxon signed-rank test) on the PET-2 scan (average SUV_{max}, 23.37 ± 25.92) than on the corresponding PET-1 scan (SUV_{max}, 18.60 ± 18.84). When we compared the signal between tracers separately, solely the difference between ^{68}Ga-PSMA-11 and ^{18}F-PSMA-1007 reached statistical significance (SUV_{max}, 16.04 ± 18.47 vs. 22.83 ± 28.12, $P = 0.01367$, 10 lesions). The differences between ^{18}F-DCFPyL and ^{18}F-PSMA-1007 (SUV_{max}, 28.2 ± 26.26 vs. 34.91 ± 36.02, $P = 0.3125$, 5 lesions), as well as ^{18}F-JK-PSMA-7 and ^{18}F-PSMA-1007 (SUV_{max}, 16.12 ± 14.81 vs. 17.38 ± 16.42, $P = 0.1641$, 9 lesions), showed a similar trend but did not reach statistical significance.

TABLE 1
Contingency Table of PSMA-RADS Results for Lesions Confirmed as True-Positive for Locoregional Relapse

		PET-2		
PET-1	PSMA-RADS	RADS 1/2	RADS 3	RADS 4/5
Reader 1	RADS 1/2	0	0	3
	RADS 3	0	6	9
	RADS 4/5	0	0	9
Reader 2	RADS 1/2	0	1	5
	RADS 3	0	4	2
	RADS 4/5	0	0	15

The PSMA-positive lesions in the 19 patients were confirmed by histology in 5 patients, by follow-up in 11 patients, and by morphologic imaging in 1 patient. Follow-up data were not available for 2 patients. Further data for verification are presented in Supplemental Table 1.

Interpretability of PSMA-Positive Lesions in Bone Marrow

We next compared the interpretability of osteomedullary PSMA-positive lesions. Intriguingly, ^{18}F-PSMA-1007 detected a significantly higher number of PSMA-positive bone marrow findings than did the other 3 tracers: although we identified 3 PSMA-positive bone marrow lesions on PET-1 (3/27 patients), ^{18}F-PSMA-1007 revealed a total of 18 PSMA-positive spots in 7 of 27 patients. Among these 7 patients, 4 patients exhibited only discrepant findings, 2 patients showed a combination of consistent and discrepant findings, and 1 patient had a concordant PSMA-positive skeletal lesion. Discordant results in the bone marrow were observed across all 3 tracers used for comparison (^{68}Ga-PSMA-11, 2 patients; ^{18}F-DCFPyL, 1 patient; ^{18}F-JK-PSMA-7, 3 patients).

The 3 PSMA-positive bone marrow lesions on PET-1 (^{68}Ga-PSMA-11: SUV_{max}, 5.18 ± 0.79) were also present on the corresponding scans with ^{18}F-PSMA-1007 (SUV_{max}, 9.82 ± 8.86). Furthermore, these 3 lesions had a morphologic correlate on the corresponding CT scan (2 patients) or on a subsequent MRI scan (1 patient).

In marked contrast, none of the 15 findings that were exclusively detected with ^{18}F-PSMA-1007 had a morphologic correlate on the corresponding CT scan. Because of this lack of a morphologic correlate on the CT scan, both readers interpreted these 15 additional PSMA-positive spots as equivocal (PSMA-RADS-3) although they had a high signal on the PET scan, with an average SUV_{max} of 7.74 ± 3.19, which was 7.07 ± 2.52 and 4.11 ± 2.91 times higher than the baseline SUV_{max} measured in the femoral head and in the thoracic aorta, respectively. This discrepancy resulted in a significant difference in PSMA-RADS categories between PET-1 and PET-2 ($P = 1.2893 \times 10^{-8}$, Freeman–Halton extension of the Fisher exact test) and a significantly higher rate of equivocal findings ($P = 0.0006$, Fisher exact test). These lesions were subsequently double-checked through contrast-enhanced MRI. All of these MRI scans were interpreted as showing no suggestive findings in the bone marrow regions.

DISCUSSION

Our direct comparison of a first PET scan with ^{68}Ga-PSMA-11, ^{18}F-DCFPyL, or ^{18}F-JK-PSMA-7 with a second PET scan with ^{18}F-PSMA-1007 led to 3 major observations.

First, ^{18}F-PSMA-1007 increased the readers' confidence in interpreting locoregional PSMA-avid lesions near the ureter, the bladder, or the urethra as tumor tissue when the previous PET scan with ^{68}Ga-PSMA-11, ^{18}F-DCFPyL, or ^{18}F-JK-PSMA-7 was read as equivocal. Furthermore, ^{18}F-PSMA-1007 PET imaging decreased the frequency of equivocal interpretations (routine diagnostics, reader 1) or false-benign results (reader 2). Possible explanations are the lower background noise of ^{18}F-PSMA-1007 in the urinary tract and the higher signal of ^{18}F-PSMA-1007 in the locoregional lesions. Although we observed this trend for all 3 tracers used for comparison, the difference in ^{18}F-PSMA-1007 signal reached statistical significance solely in comparison to ^{68}Ga-PSMA-11 (applies to 16/27 patients in our study cohort), suggesting that the ^{18}F label with its higher activity dose contributed more to our observation than ligand-specific factors.

Second, where the PET scan with ^{68}Ga-PSMA-11, ^{18}F-DCFPyL, or ^{18}F-JK-PSMA-7 was completely PSMA-negative in the pelvis, an additional PET scan with ^{18}F-PSMA-1007 did not reveal any additional locoregional PSMA-positive lesions. Because all PSMA tracers examined in this study bind to the same protein domain, imaging with a second PSMA tracer cannot compensate for a lack of PSMA overexpression.

Third, surprisingly and although not the primary goal of this study, we found that ^{18}F-PSMA-1007 exhibited a higher rate of unspecific focal bone marrow uptake than did ^{68}Ga-PSMA-11, ^{18}F-DCFPyL, and ^{18}F-JK-PSMA-7. Since these additional bone marrow foci lacked morphologic correlates in the corresponding low-dose CT scans, both readers interpreted these additional lesions as equivocal (PSMA-RADS-3). The subsequent skeletal MRI scans were not suggestive. We observed discrepant skeletal findings in 6 of our 27 patients (22%). Our results are concordant with a recent study that reported a higher rate of PSMA-positive bone marrow lesions in 102 patients examined with ^{18}F-PSMA-1007 than in a matched-pair cohort examined with ^{68}Ga-PSMA-11 (*13*). However, in contrast to our study, these 102 patients received a scan with ^{18}F-PSMA-1007 only and were not examined with a second PSMA tracer. In light of the results of our study, CT-negative bone marrow findings detected with ^{18}F-PSMA-1007 require validation by MRI scans. The importance of clinical follow-up is independent of the PSA value, since even patients with biochemical recurrence and low PSA levels occasionally have PSMA-positive bone marrow metastases, as recently reported for ^{18}F-DCFPyL (*14*).

This study had some limitations. Our direct comparison between ^{68}Ga-PSMA-11, ^{18}F-DCFPyL, and ^{18}F-JK-PSMA-7 in PET-1 and ^{18}F-PSMA-1007 in PET-2 was not designed as a prospective clinical trial. Readers were not masked to the PSMA PET tracer, and we observed a relevant interobserver variability between readers 1 and 2 in the interpretation of PET-1 (weighted Cohen $\kappa = 0.49$). Our observations were focused on a highly selected cohort of 27 patients from an overall group of 668 patients (4.0%) who underwent PSMA PET/CT during the recruitment period of 1 y. A second PSMA PET scan with ^{18}F-PSMA-1007 was performed only when clinically indicated, mainly because of an equivocal or negative interpretation of the first PET scan. For this reason, our cohort was relatively small. Establishing a preferred PSMA tracer will require independent validation in larger cohorts.

CONCLUSION

Our study suggests that the choice of the right PSMA tracer depends on the clinical context. ^{18}F-PSMA-1007 may increase confidence in interpreting small locoregional lesions adjacent to the urinary tract and may thus help to reduce equivocal interpretations in selected patients. However, ^{18}F-PSMA-1007 exhibits unspecific PSMA tracer accumulation in the bone marrow in a relevant number of patients. Thus, skeletal lesions detected with ^{18}F-PSMA-1007 require verification such as through MRI or simultaneous PET/MRI. Imaging with ^{18}F-PSMA-1007 may therefore be applicable primarily to patients with a high probability of locally restricted disease or as a follow-up test in cases with equivocal findings adjacent to the urinary tract. When one is searching for distant metastases, particularly in the bone marrow, ^{68}Ga-PSMA-11, ^{18}F-DCFPyL, or ^{18}F-JK-PSMA-7 may be more suitable because of their higher specificity in the bone marrow.

DISCLOSURE

Bernd Neumaier, Philipp Krapf, Boris Zlatopolskiy, and Alexander Drzezga have applied for a patent on ^{18}F-JK-PSMA-7. No other potential conflict of interest relevant to this article was reported.

KEY POINTS

QUESTION: Does ^{18}F-PSMA-1007 exhibit a higher sensitivity for subtle differences near the urinary tract than other established PSMA tracers?

PERTINENT FINDINGS: ^{18}F-PSMA-1007 facilitated the interpretability of locoregional PSMA-positive lesions, compared with the other established PSMA PET tracers. The number of equivocal and false-benign interpretations decreased significantly for 2 independent readers. However, ^{18}F-PSMA-1007 exhibited a substantial number of unspecific findings in the bone marrow.

IMPLICATIONS FOR PATIENT CARE: Because of the high tracer signal of the unspecific skeletal ^{18}F-PSMA-1007 spots, reader training alone will not solve this problem. Thus, skeletal lesions detected with ^{18}F-PSMA-1007 PET without a correlate in the corresponding CT scan require an additional examination, such as MRI or simultaneous PET/MRI.

REFERENCES

1. Giesel FL, Hadaschik B, Cardinale J, et al. F-19 labelled PSMA-1007: biodistribution, radiation dosimetry and histopathological validation of tumor lesions in prostate cancer patients. *Eur J Nucl Med Mol Imaging.* 2017;44:678–688.
2. Giesel FL, Knorr K, Spohn F, et al. Detection efficacy of ^{18}F-PSMA-1007 PET/CT in 251 patients with biochemical recurrence of prostate cancer after radical prostatectomy. *J Nucl Med.* 2019;60:362–368.
3. Rahbar K, Afshar-Oromieh A, Bögemann M, et al. ^{18}F-PSMA-1007 PET/CT at 60 and 120 minutes in patients with prostate cancer: biodistribution, tumour detection and activity kinetics. *Eur J Nucl Med Mol Imaging.* 2018;45:1329–1334.
4. Dietlein M, Kobe C, Kuhnert G, et al. Comparison of [^{18}F]DCFPyL and [^{68}Ga]Ga-PSMA-HBED-CC for PSMA-PET imaging in patients with relapsed prostate cancer. *Mol Imaging Biol.* 2015;17:575–584.

5. Dietlein F, Kobe C, Neubauer S, et al. PSA-stratified performance of ^{18}F- and ^{68}Ga-PSMA PET in patients with biochemical recurrence of prostate cancer. *J Nucl Med.* 2017;58:947–952.
6. Dietlein F, Hohberg M, Kobe C, et al. A novel ^{18}F-labeled PSMA ligand for PET/CT imaging of prostate cancer patients: first-in-man observational study and clinical experience with ^{18}F-JK-PSMA-7 during the first year of application. *J Nucl Med.* July 19, 2019 [Epub ahead of print].
7. Zlatopolskiy BD, Endepols H, Krapf P, et al. Discovery of ^{18}F-JK-PSMA-7, a novel PET-probe for the detection of small PSMA positive lesions. *J Nucl Med.* 2019;60:817–823.
8. Giesel FL, Will L, Lawal I, et al. Intraindividual comparison of ^{18}F-PSMA-1007 and ^{18}F-DCFPyL PET/CT in the prospective evaluation of patients with newly diagnosed prostate carcinoma: a pilot study. *J Nucl Med.* 2018;59:1076–1080.
9. Eder M, Schafer M, Bauder-Wust U, et al. ^{68}Ga-complex lipophilicity and the targeting property of a urea-based PSMA inhibitor for PET imaging. *Bioconjug Chem.* 2012;23:688–697.
10. Chen Y, Pullambhatla M, Foss CA, et al. 2-(3-{1-carboxy-5-[(6-[^{18}F]fluoro-pyridine-3-carbonyl)-amino]-pentyl}-ureido)-pentanedioic acid, [^{18}F]DCFPyL, a PSMA-based PET imaging agent for prostate cancer. *Clin Cancer Res.* 2011;17:7645–7653.
11. Eiber M, Herrmann K, Calais J, et al. Prostate cancer molecular imaging standardized evaluation (PROMISE): proposed miTNM classification for the interpretation of PSMA-ligand PET/CT. *J Nucl Med.* 2018;59:469–478.
12. Rowe SP, Pienta KJ, Pomper MG, Gorin MA. Proposal for a structured reporting system for prostate-specific membrane antigen-targeted PET imaging: PSMA-RADS version 1.0. *J Nucl Med.* 2018;59:479–485.
13. Rauscher I, Krönke M, König M, et al. Matched-pair comparison of ^{68}Ga-PSMA-11 and ^{18}F-PSMA-1007 PET/CT: frequency of pitfalls and detection efficacy in biochemical recurrence after radical prostatectomy. *J Nucl Med.* June 28, 2019 [Epub ahead of print].
14. Wondergem M, Jansen BHE, van der Zant FM, et al. Early detection with ^{18}F-DCFPyL PET/CT in 248 patients with biochemically recurrent prostate cancer. *Eur J Nucl Med Mol Imaging.* 2019;46:1911–1918.